# Variable processing shifts during perceptual acceleration: Evidence from temporal integration

Michael J. Wolff[1] & Elkan G. Akyürek[2]

[1] Ernst Strüngmann Institute (ESI) for Neuroscience in Cooperation with Max Planck Society, Frankfurt, Germany

[2] Department of Experimental Psychology, University of Groningen, The Netherlands

12/02/2025

Word count: 7774

Address correspondence to:
Elkan Akyürek
Department of Experimental Psychology, University of Groningen
Grote Kruisstraat 2/1, 9712 TS Groningen, The Netherlands
Email: e.g.akyurek@rug.nl
Telephone: +31 (0)50 3636406

## Abstract

The perception of a stimulus can be accelerated by another that precedes it. Research to date has focused on quantifying this acceleration, and localizing it in the chain of perceptual and cognitive processes that are involved. This is challenging, because these processes may interact unexpectedly, and because traditional (univariate) analyses of brain activity and behaviour may conflate processes with the representations they act on. By using multivariate pattern analysis of EEG data from a missing element task, designed to measure the visual temporal integration of two successive stimulus displays, we were able to track the representation associated with the integrated percept. We manipulated the delay between our displays, and observed commensurate acceleration of the resultant integrated representation. Furthermore, regardless of the delay, we found that although processing was already accelerated during the earliest processing stages at around 100ms after stimulus onset, intermediate stages, at around 200ms, were even more accelerated. In contrast, later processing stages, at around 400ms, again showed less acceleration. The results thus suggest that perceptual acceleration during temporal integration is nonlinear, and that some time that is gained at one moment in the process can be lost again at another.



**Keywords**: visual perception; perceptual acceleration; temporal integration; electroencephalography; multivariate pattern analysis

# 1 Introduction

We live in the past. As we experience the world around us, our impressions inevitably lag behind the physical reality, because it takes some time to route a signal from our eyes and through the brain. Evolution has surely minimized that delay, but it still takes approximately 120-150 ms to determine basic properties of an unfamiliar natural scene, such as to determine whether it contains an animal or not (Cichy, Pantazis, & Oliva, 2014; Kirchner & Thorpe, 2006; Thorpe, Fize, & Marlot, 1996; VanRullen & Thorpe, 2001). Prior to that small but persistent delay, higher-level awareness of the contents of the scene is considered to be virtually absent. So, we have no choice but to wait until the sensory signal has traversed through the necessary perceptual and cognitive processing steps, before we can actually react to it.

The idea that perceptual and cognitive functions necessarily take a certain amount of time to complete is well-supported. How much time is needed exactly nevertheless varies. Somewhat trivially, it depends on the complexity of the task. Grouping stimuli together in space will likely be faster if those stimuli are all regularly spaced and sized, than when they are not, for example. Apart from that, processing a given stimulus may also take less time, if circumstances allow for increased readiness. Research to date has shown several ways to accelerate processing in this manner. Explicit cues about the where and when of upcoming stimuli can help to prepare for their arrival, as can implicit temporal expectancies generated by systematicities in their onset.

The Posner cueing task is arguably one of the most basic tasks that provides advance knowledge about the location of an upcoming target stimulus to its participants (Posner, 1980). In this task, a target stimulus appears on the left of right side of the screen, and is preceded by a cue that directs attention to either location. A valid cue reduces the time needed to respond to the target, compared to conditions in which no advance information is provided, or an invalid cue is given. Neurophysiologically, this is accompanied by amplitude (but not latency)

modulations of early ERP components, such as the P1 and N1 (Mangun, 1995; Mangun & Hillyard, 1990). Thus, spatial cueing seems to boost the electrophysiological response to target stimuli, and accelerate the associated behavioural response. Similarly, cues about the timing (i.e., the onset) of a target stimulus can provide perceptual processing benefits. Coull and Nobre (1998) presented (symbolic) cues that were predictive of the onset of a target stimulus, and found that target reaction times were decreased for valid cues. Using a similar temporal and spatial cueing design, Griffin, Miniussi, and Nobre (2002) found that apart from reduced reaction times to valid cues, cueing caused several ERP component amplitude differences. They also observed a reduction of the latency of the P3 due to temporal cues specifically.

More implicit expectations about the onset of a stimulus are also known to facilitate its processing. For instance, stimuli that arrive in sync with a rhythm established by preceding stimuli are more accurately perceived (Jones et al., 2002; Mathewson et al., 2010). Electrophysiologically, this is expressed by synchronization of the CNV component to the expected onset, and modulation of alpha and beta band oscillations (Praamstra et al., 2006; Rohenkohl & Nobre, 2011). Anticipation of a target can build up even without a rhythmic component, during blank delay intervals ("foreperiods") prior to target onset. This build-up of anticipation is thought to follow a so-called hazard function, which reflects the probability of the target appearing, given that it has not yet occurred (Luce, 1986). Behavioural evidence has suggested that such temporal preparation may increase the speed at which sensory evidence accumulates, or allow for an earlier onset of this process (Seibold et al., 2011; Vangkilde, Coull, & Bundesen, 2012; see also Jepma, Wagenmakers & Nieuwenhuis, 2012). Electrophysiological studies have also provided direct evidence for foreperiod-dependent perceptual acceleration. In one auditory study, the latency of the N2 was reduced (Seibold, Fiedler, & Rolke, 2011), while in a visual analogue, decreased N1 and N2pc latencies were found (Seibold & Rolke, 2014).

An important question about perceptual acceleration is when it acts, that is, what perceptual and/or cognitive (sub-) processes it affects. To specify its locus in the chain of processing that underlies perception and cognition, one approach is to divide this chain of processing into distinct, independent stages or modules. This is made explicit in additive factors logic (Donders, 1868; Sternberg, 1969; 2001). Herein each stage is conceptualized as an independent computation, transforming input to output, upon which acceleration may act, reducing the time needed to complete that transformation, without affecting any other processing stage. The relationship between different stages is nevertheless summative, so that subsequent computations in the perceptual and cognitive chain will commence sooner, until eventually the behavioural response is also quickened. Next to traditional reaction time measures, the tenets of this "mental chronometry" can also be assessed neurophysiologically (Linden, 2007).

Nevertheless, it can be difficult to prove independence between different processing stages in practice, and under- or over-additive effects may emerge, suggesting concurrent modulation of multiple stages. Such concurrency has indeed been observed in dual-task situations, where the processing of multiple (conflicting) stimuli is required simultaneously (Ridderinkhof et al., 1995), and where multiple subtasks need to be chained (e.g., Sackur & Dehaene, 2011), but also in single-task foreperiod studies (e.g., Los & Schut, 2008). One way in which stage conceptualizations can deal with such variability is by using neurophysiological markers ("bumps") to define stages, and allowing temporal variation within each stage (Anderson et al., 2016; van Maanen, Portoles, & Borst, 2021; Vidaurre, Cichy, & Woolrich, 2021; Vidaurre et al., 2019), although this may thereby detract to some degree from the idea of a serial processing chain, and make it harder to pinpoint modulatory factors therein.

A further complication in the effort to track perceptual acceleration in the brain is that it is difficult to relate traditional electrophysiological measures to behavioural effects that

emerge at the end of the processing chain. For example, how does a change in amplitude, or even a latency shift, of a given ERP component translate into a faster behavioural response (for a similar argument, see Jepma, Wagenmakers & Nieuwenhuis, 2012)? This difficulty is partly due to the generic nature of the measures themselves. For example, an ERP component may reflect attentional processing of stimuli, but it generically reflects that cognitive process as well as the representations it acts on. However, by combining time-sensitive EEG measures with multivariate pattern analysis (MVPA), which allows tracking of stimulus-specific representations, it is possible to put a timestamp on the flow of information in the brain (Marti, King, & Dehaene, 2015), and track perceptual acceleration. This is what we set out to do here.

### 1.1 The current study

We used a missing element task to assess perceptual acceleration. The missing element task is traditionally used to measure temporal integration, and entails the presentation of two successive stimulus arrays. Together, the arrays fill up a grid of stimuli, apart from a single location in the grid that remains empty. If this location is found by the observer, this is evidence that the successive arrays were temporally integrated. The rapid, spatially constrained, yet non-overlapping presentation of the two displays also provides a situation in which the perception of the second display may be facilitated by the appearance of the first, in a low-level stimulus-driven manner. Although the present study is agnostic as to the underlying mechanism, one might suppose that the rapid succession of the stimulus displays may cause coincidental neuronal activity, leading to synaptic facilitation through residual elevation of presynaptic $Ca^{2+}$ (Markram et al., 1997; Zucker & Regehr, 2002). Alternatively, processing of the first stimulus display in higher-order cells may facilitate processing of the second display in lower-order cells, through back-projections (Friston, 2005; Palmer et al., 2015; Summerfield & Egner, 2009).

We manipulated the stimulus onset asynchrony (SOA) between the displays in our missing element task, measured the EEG, applied multivariate pattern analysis (MVPA) to decode the location of the missing element, and compared its occurrence in time between conditions by means of cross-temporal generalization. To preview the results, we found evidence for accelerated perceptual processing during temporal integration, but also observed that this acceleration varied over time as the missing element was being processed in the brain, such that initial gains were partially lost again later in that process.

# 2 Methods

## 2.1 Participants

Twenty-four first year psychology students of the University of Groningen (9 female, mean age 21 years, range 18-28 years) were included in the analyses. Eight additional participants failed to meet the previously set inclusion criterion (80 % accuracy on the SOA 0/no integration condition), and their data was discarded during collection. Participants received course credits for participation and gave written informed consent. The study was approved by the ethical committee of the Psychology department of the University of Groningen (approval number: 16340-S-NE).

## 2.2 Apparatus and Stimuli

Stimuli were controlled and generated with Psychtoolbox, a freely available toolbox for Matlab (Kleiner et al., 2007), and presented on a 19-inch (48.3 cm) CRT screen running at 200 Hz refresh rate and a resolution of 640 by 480 pixels. Responses were made with a conventional computer mouse. Participants were seated at approximately 64 cm from the monitor. The stimuli consisted of black squares (0.72°) arranged in a 6 by 6 grid (7.92°) in the centre of the screen. The empty spaces between squares were the same size as the squares themselves

(0.72°). A black fixation cross (0.97°) and a grey background (RGB = 150, 150, 150) were maintained throughout the trials.

**2.3 Procedure**

Each trial began with the presentation of a fixation cross. After 800 ms, 35 out of 36 black squares, arranged on a 6 by 6 grid, were presented either at the same time (SOA 0 ms), or across two successive displays, for 20 ms each, with an interstimulus interval (ISI) of 10, 25, or 40 ms (SOA 30, 45, or 60 ms). Participants were instructed to locate the one missing square, which could be anywhere within the inner 4 by 4 grid, and of which they were made aware beforehand. Note that in order to detect the missing square, both displays need to be temporally integrated by the perceptual system, which is more difficult at longer SOAs (Di Lollo, 1977; Hogben & Di Lollo, 1974). The response screen was presented 1,100 ms after the onset of the first display, and consisted of the whole grid of squares. Participants used the mouse cursor to click on the square that they thought was previously missing. Immediately after their response, the correct square flashed in green, and, if incorrect, the chosen square in red. Participants completed 1,056 trials in total, over a course of approximately 75 minutes, including breaks. See Figure 1a for a trial schematic.

No integration (SOA 0) trials made up 27%, SOA 30 trials made up 27 %, and SOA 45 and SOA 60 made up 36% and 9% of all trials, respectively. SOA 45 made up the largest proportion of trials due to the anticipated difficulty of this condition. Of the most difficult condition of SOA 60, only a small number of trials was included in the experiment. These served merely to confirm the expected decrease in accuracy as a function of SOA due to temporal integration eventually breaking down, as has previously been observed (e.g., Akyürek, Schubö, & Hommel, 2010), and this SOA was excluded from all neurophysiological analyses.

## 2.4 Electrophysiological recording and pre-processing

The EEG signal was acquired from 59 Ag/AgCls sintered electrodes laid out according to the extended international 10-20 system, with two additional electrodes placed on the mastoids. Another electrode, placed above the sternum, was used as ground. Four electrodes placed above and below the left eye and on the temples recorded the bipolar EOG signals. Offline, the data were re-referenced to the average of both mastoid electrodes and filtered with a 0.05 Hz high-pass and a 40 Hz low-pass filter. The data were epoched relative to the onset of the first display (-250 ms to 1100 ms) and baseline corrected using the mean signal from -250 to 0 ms relative to Display 1 onset. Noisy trials and trials containing ocular artefacts were identified by visually inspecting the EEG and EOG signal and removed from the analyses.

## 2.5 Location decoding

We were interested in the time-course of the location code of the missing square in the EEG signal. We used Mahalanobis distance (De Maesschalck, Jouan-Rimbaud, & Massart, 2000) to test if the signal contained information about the location at any one point throughout the trial. Only the 24 posterior channels were included in the decoding analyses (P7, P5, P3, P1, Pz, P2, P4, P6, P8, PO7, PO3, POz, PO4, PO8, O1, Oz, O2, P9, PO9, O9, Iz, O10, PO10, and P10). The EEG data was smoothed with a Gaussian smoothing kernel (SD=10 ms) along the time dimension, and mean centred across channels prior to analysis. Using an 8-fold cross-validation approach, the trial-wise Mahalanobis distances between train trials and the left-out test-trials was computed at each time-point separately. The covariance matrix was computed at each time-point using all train trials with a shrinkage estimator (Ledoit & Wolf, 2004). This procedure was repeated 50 times, each time randomly partitioning the data into 8 folds. Same-location distances were subsequently subtracted from the average of all different-location

distances, such that a positive "distance difference" represents a shorter distance between trials that had the same missing square locations than between trials that had different locations (Wolff, Ding, Myers, & Stokes, 2015), suggesting that the electrophysiological signal contains location-specific information.

## 2.6 Cross-temporal decoding

We were interested in the neural dynamics of the processing of the missing square. Instead of training and testing the classifier on the same time-points as described above, in cross-temporal decoding analyses, the classifier is trained and tested on all possible time-point combinations, resulting in a full cross-temporal decoding matrix (King & Dehaene, 2014). The cross-temporal dynamics were tested for significance using the same method as in Myers and colleagues (2015): The decodability at each cross-temporal time-point $t_{x,y}$ to the corresponding time-points on the diagonal ($t_{x,x}$ and $t_{y,y}$). A significant difference in both was taken as evidence for dynamic coding. A cluster-based permutation test was used to correct for multiple comparisons.

Finally and most importantly, we wanted to test to what extent the processing of the missing square location is temporally shifted when the necessary visual information is not presented simultaneously, as in the SOA 0 condition, but spread across two discrete displays, as in the SOA 30 and SOA 45 conditions. To do so, we trained the classifier on each time-point separately in the SOA 0 condition, and tested it on all time-points in both the SOA 30 and SOA 45 conditions, obtaining a full cross-temporal decoding matrix between conditions.

## 2.7 Quantifying the temporal shift

We wanted to quantify the possible temporal shift obtained from the cross-temporal and cross-condition decoding matrices, where the classifier was trained on the no-integration

condition (SOA 0) and tested on each temporal integration (SOA 30 and 45, see above). To quantify this shift, we developed an analysis that assumes that a dynamic cross-temporal decoding profile is symmetric around the true temporal offset. First, to obtain a more fine-grained temporal estimate, the cross-temporal decoding matrices were "up-sampled" using 2D spline interpolation, estimating the temporal resolution at 2048 Hz (from the original 1024 Hz). Note that this step is not crucial for the analysis or results. All results are qualitatively the same and quantitively very similar without temporal interpolation. Next, the dynamics of the decoding matrices were normalized at each time-point by z-scoring the decoding values across both the x and y axes of the matrices and then averaging them. Finally, a centred 50 ms sliding window approach was used to determine the temporal shift. At each time-point along the diagonal (from 90 ms, the onset of reliable decoding in the SOA 0 condition, to 500 ms), the average of all decoding values in the upper triangle were subtracted from the average of the lower triangle. This sliding window was moved up and down the training and testing axes of the decoding matrix. Zero difference at a specific offset suggests that the cross-temporal decoding window is symmetrical at this offset, whereas a positive or negative difference provides evidence for a temporal shift in the corresponding direction.

The "shift score" was computed using the following formula:

$$s_{t,o} = \frac{\big(L(t_{trn}, t_{tst} + o) - U(t_{trn}, t_{tst} + o)\big) + \big(L(t_{trn} - o, t_{tst}) - U(t_{trn} - o, t_{tst})\big)}{2}$$

$$s_{t,o} = \frac{(L1_{t,o} - U1_{t,o}) + (L2_{t,o} - U2_{t,o})}{2}$$

where $t_{trn}$ and $t_{tst}$ are the time-points along the training and testing axis, respectively, both relative to the onset of the first display ($t_{trn} = t_{tst}$), $U$ and $L$ are the means of the upper and lower triangle of the 50ms sliding window, respectively, $o$ is the temporal offset of the sliding window (in ms) relative to $t$, and $s$ is the shift score.

### 2.8 Identifying distinct stages of location processing

The time-course of decoding and the cross-temporal decoding matrix of the no-integration condition were compared to the ERP, to identify different stages in processing of the location of the missing element. Stages were characterized on the basis of the correspondence observed between ERP component amplitude, decoding accuracy, and (switches between) periods of dynamic and stable coding. The identification of these stages was not necessarily meant to strictly delineate separable or independent processes, but to provide a handle on different moments within the perceptual process.

### 2.9 Significance testing

We used non-parametric permutation tests for all statistical analyses. In subject analyses, for each subject, the sign of the decoding time-series data was randomly flipped at each time-point 5,000 times. The resulting null-distribution was used to derive the *p*-value. Cluster-based permutation tests were used to correct for multiple comparisons across the time-dimension(s) using 5,000 permutations, with a cluster-forming threshold of $p < 0.05$. Statistical significance was set at $p < 0.05$. All tests were two-sided. Group-level analyses were used to estimate the temporal shift at each specific processing stage (detailed below) and SOA condition. The mean temporal shift values were sampled with replacement from each time-window of interest and the shift was computed 5,000 times. The resulting distribution was used to compute the 95% confidence interval.

Differences between SOAs and processing stages were also tested on the group level by randomly flipping the condition labels of each subject with 0.5 probability, before computing the mean difference 5,000 times. The null distribution was used to calculate the proportion of permutations more extreme than the actual group-level difference. Statistical significance was set at $p < 0.05$. Tests between SOA conditions were one-sided, testing

specifically if the temporal shift in the SOA 45 condition was larger than in the SOA 30 condition. The *p*-values of all possible pairwise differences between processing stages were Bonferroni-corrected for multiple comparisons and were two-sided.

## 3 Results

### 3.1 Behavioural

Figure 1b shows a clear negative effect of increasing SOA on the behavioural accuracy of locating the missing square. This suggests that the two displays are less likely to be temporally integrated at longer SOAs, leading to worse performance, which replicates previous findings (e.g., Akyürek, Schubö, & Hommel, 2010; Di Lollo, 1977).

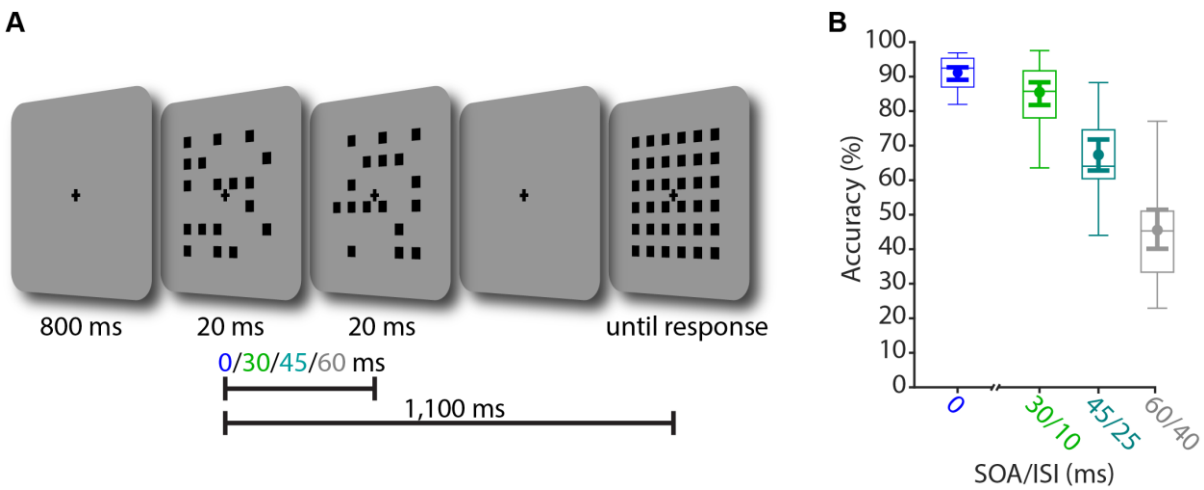


**Figure 1. Task structure and behavioural performance**

**(A)** Trial schematic of the missing element task. After the presentation of an initial fixation cross, 35 out of 36 squares on a 6 by 6 grid were presented either at the same time (SOA 0 ms) or across two successive displays (SOA 30, 45, and 60 ms). The response screen was presented after a short delay and participants clicked on the square they thought was previously missing. **(B)** Boxplots show task accuracy as a function of SOA condition. Centre lines indicate the median; box outlines show 25$^{th}$ and 75$^{th}$ percentiles, and whiskers indicate 1.5x the interquartile

range. The superimposed filled circles and error bars indicate means and the 95% C.I. of the means, respectively.

### 3.2 Distinct stages of location processing

We used the SOA 0 condition as a "template" to define the time-windows of individual processing stages, and to test the neural dynamics of location processing. The decoding time-course showed a significant cluster from 91 ms to 1,100 ms (end of epoch), relative to display onset ($p < 0.001$, cluster-corrected), providing evidence that the location of the missing square was decodable from the EEG shortly after stimulus presentation (Fig. 2a). The cross-temporal decoding matrix showed that approximately 140 ms after stimulus onset training and testing trials cross-generalized significantly, while at the same time providing evidence for a highly dynamic code from decoding onset until approximately 500 ms after onset (decoding cluster: $p < 0.001$; dynamic coding cluster: $p < 0.001$, both cluster-corrected; Fig. 2b). Visual inspection of the 1-dimensional and 2-dimensional decoding time-courses, in conjunction with the significant clusters of decoding and dynamic coding, suggested four distinct processing stages, which corresponded well with the averaged evoked potentials (Fig. 2c).

1. An early location-specific response from approximately 90 to 140 ms, which did not cross-generalize with any subsequent time-points. The decoding time-course overlapped with the P1, which is known to be modulated by early attentional filtering and stimulus selection (Hillyard et al., 1998), and which originates in V2 (Woldorff et al., 1997).
2. High decodability from 140 to 300 ms, overlapping with the time-course of the N1 and N2, likely reflecting the attentional shift towards the location of the missing square (e.g., Patel & Azzam, 2005), and spatial grouping (Akyürek, Schubö, & Hommel, 2010).

3. Highly dynamic location decoding from 300 to 500 ms, overlapping with the time-course of the P3, likely reflecting the consolidation of the missing square location in working memory, and processes related to response selection (Polich, 2007; Verleger et al., 2005).
4. Stable and relatively low decoding from 500 to 1,100 ms (end of epoch), likely reflecting the continuous maintenance of the missing square location in working memory, possibly related to the CDA (Akyürek et al., 2017; Vogel & Machizawa, 2004).

Since we were interested in the temporal shift of the dynamic brain states between no-integration and integration, we focused on the dynamic time-window up to 500 ms after stimulus presentation for all subsequent analyses, excluding the stable maintenance period.

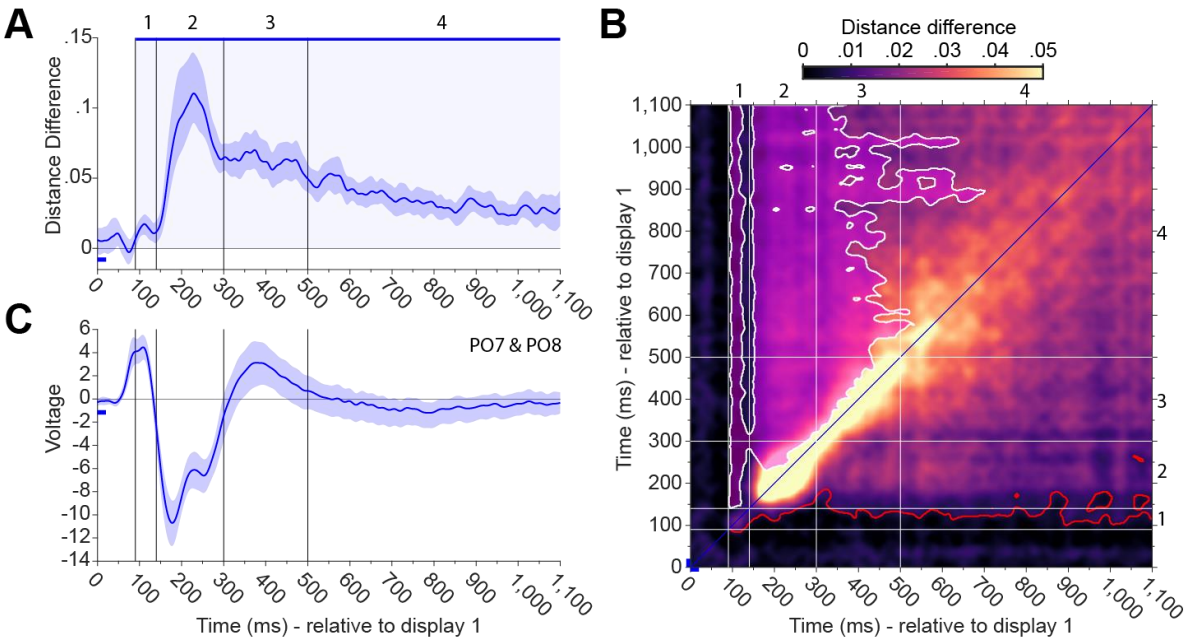


**Figure 2. Identifying distinct processing stages**

**(A)** Decoding time-course of the location of the missing square in the SOA 0 condition. Blue bar on top indicates significant decoding ($p < 0.05$, cluster-corrected). Blue bar on the bottom left indicates Display 1 presentation. Error-shading indicates the 95% C.I. of decoding accuracy. Black vertical lines and numbers indicate distinct processing stages (see text). **(B)**

Cross-temporal decoding matrix of the SOA 0 condition. The white outline depicts time-points of significantly lower decoding than for both equivalent time-points along the diagonal, providing evidence for dynamic coding ($p < 0.05$, cluster-corrected). The red outline indicates time-points of significant decoding ($p < 0.05$, cluster-corrected). **(C)** Average evoked potential from the electrodes PO7 and PO8 with 95% C.I. (blue shading).

### 3.3 Exemplifying "shift score" computation on SOA 0

We quantified the mid-point of the cross-temporal decoding matrix relative to the diagonal by computing the shift score. Here we demonstrate this analysis on the cross-temporal decoding matrix of the SOA 0 condition, where we do not expect a systematic deviation from diagonal, since both training and testing come from the same SOA 0 condition. The method is described above ("Quantifying the temporal shift") and illustrated in Figure 3. A significance test on the shift-score matrix reveals one negative and one positive cluster of shift-score values ($p < 0.001$, cluster-corrected; Fig. 3b). Neither of the clusters cross the 0 line, demonstrating that while there is no evidence for a temporal shift when training and testing at the same time-points, the shift-score analysis is sensitive enough to pick up the asymmetry of the decoding matrix when separating training and testing by as little as ~5 ms. The 0 ms offset was explicitly tested for significant shift-scores. As expected, no significant clusters were detected ($p > 0.2$, cluster-corrected; Fig. 3c).

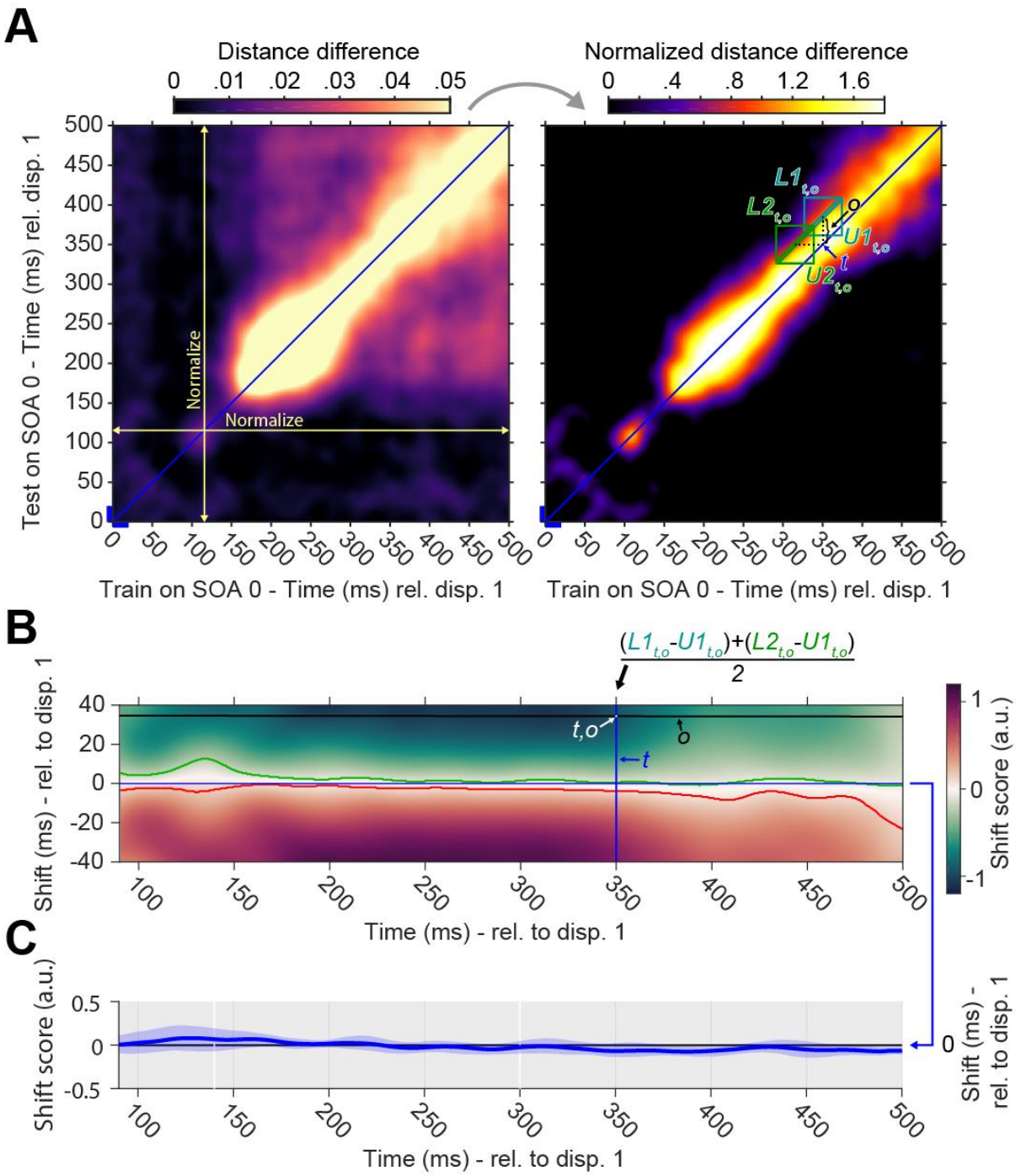


**Figure 3. Demonstration of "shift score" computation**

**(A)** Cross-temporal decoding matrix of the SOA 0 condition (left). Yellow lines visualize normalization across cross-temporal time-dimension. Normalized decoding matrix by z-scoring decoding values along the cross-temporal time-dimensions (right). Computation of shift score at a specific time (*t*) and temporal offset (*o*) is illustrated. **(B)** Shift scores with temporal offsets from -40 to 40 ms. Negative values suggest higher decodability at shorter

offsets, positive values suggest higher decodability at longer offsets. Green and red outlines depict significantly negative and positive shift-score clusters ($p < 0.05$), respectively. **(C)** Shift score at 0 ms temporal offset with 95 % C.I. No evidence of significant deviation was found ($p > 0.2$, cluster-corrected), suggesting that the neural dynamics are centred at 0 (as expected).

### 3.4 Temporally shifted neural dynamics of location processing during temporal integration

The neural dynamics of missing square location processing in the SOA 0 condition cross-generalized significantly with both temporal integration conditions ($p < 0.001$ of both cross-temporal decoding clusters; Fig. 4a & b), with similar neural dynamics across the whole time-window as SOA 0 (see Fig. 3a). This suggests that the neural representations of location information processing are qualitatively similar, regardless of whether that information needs to be temporally integrated first or not. However, a temporal shift seemed to be present in both temporal integration conditions, as the decoding dynamics were not symmetrical along the diagonal (training at testing at the same time-points, relative to Display 1 onset).

Two clusters of significant shift-scores were present in the SOA 30 condition, one negative and one positive (both $p < 0.001$, cluster-corrected; Fig. 4c). For the most part, the point of decoding symmetry (shift-score = 0) was wedged between the onset of Display 1 (0 ms) and Display 2 (30 ms), constituting evidence for perceptual acceleration during temporal integration. A positive and negative shift-score cluster were also present in the shift score matrix of the SOA 45 condition (both $p < 0.001$, cluster-corrected; Fig. 4d). Like SOA 30, the point of symmetry was largely between the onsets of the first and second display, though the acceleration during integration seemed to diminish towards the end of the dynamic time-window.

We explicitly tested if there was evidence for a temporal shift at the temporal onsets of the first (0 ms) and the second display (30/45 ms) in both temporal integration conditions. In the SOA 30 condition, this revealed a significant negative shift-score cluster from 90 to 373 ms at a temporal offset of Display 2 onset ($p < 0.001$, cluster-corrected; Fig. 4e, top), providing evidence for a temporal offset of the neural dynamics that is less than the SOA between displays (30 ms). Two positive shift-score clusters were present at 0 ms temporal offset (90 to 132.5 ms, $p = 0.043$; 229 ms to 451, $p < 0.001$, cluster-corrected; Fig. 4e, bottom), indicating that location processing is delayed during temporal integration relative to Display 1 onset. The SOA 45 condition showed a similar pattern of results. One negative shift-score cluster was present at a temporal offset of Display 2 (90 to 344 ms, $p < 0.001$, cluster-corrected; Fig. 4f, top), as well as three positive clusters at 0 ms temporal offset (94.5 to 214 ms, $p < 0.001$; 254 to 370 ms, $p < 0.001$; 378 to 476.5 ms, $p = 0.004$, cluster-corrected; Fig. 4f, bottom).

In sum, when Display 2 was delayed, processing of the missing element location was also delayed, compared to the SOA 0 condition (Fig. 4e & f, bottom). However, it was not delayed as much as would be expected from the SOA (i.e., 30 or 45 ms) between displays (Fig. 4e & f, top). That means that the processing of the missing element was actually accelerated in these integration conditions.

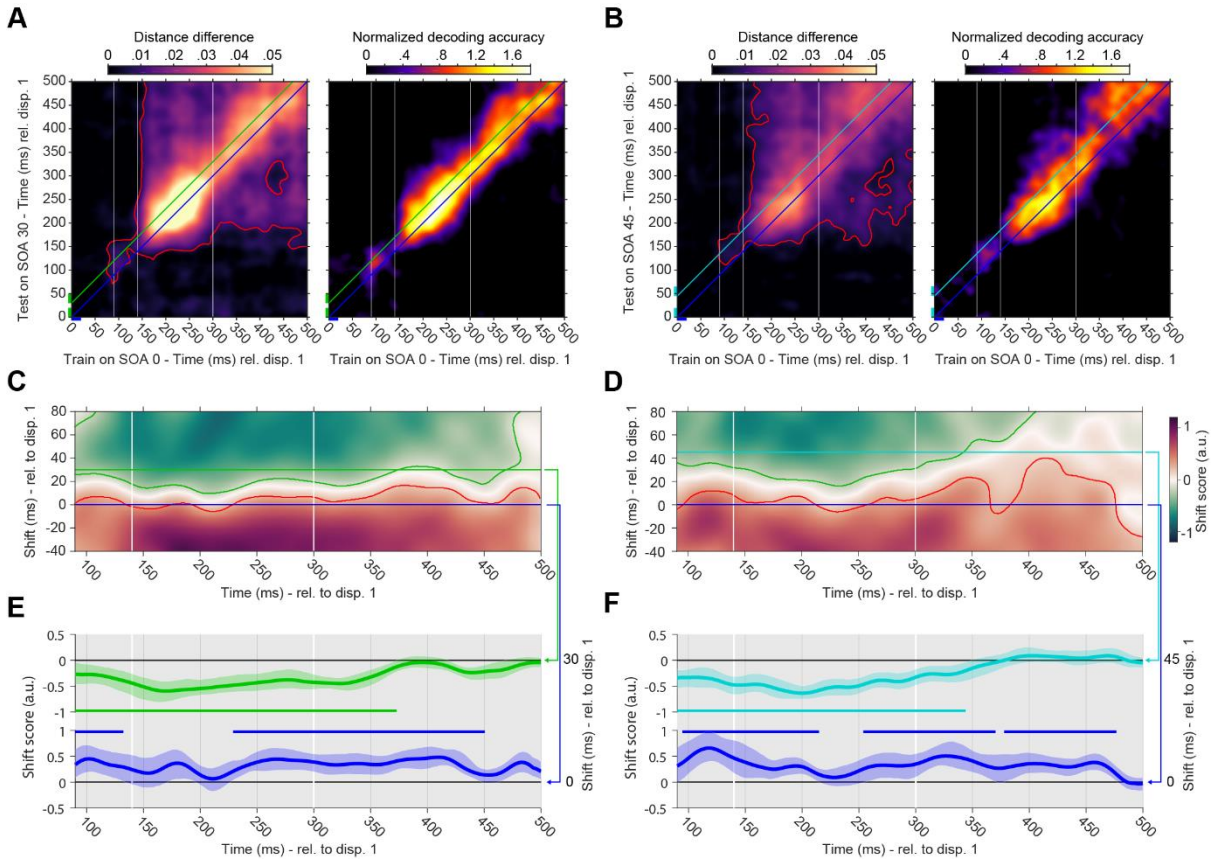


**Figure 4. Accelerated location processing during temporal integration**

**(A)** Cross-temporal generalization matrix between SOA 0 and SOA 30. White lines indicate previously defined processing stages. *Left:* The red outline indicates time-points of significant cross-generalization ($p < 0.05$, cluster-corrected). *Right:* Normalized generalization matrix. **(B)** Cross-temporal generalization matrix between SOA 0 and SOA 45. **(C)** and **(D)** Shift scores of normalized cross-temporal generalizations between SOA 0 and SOA 30, and SOA 0 and SOA 45, respectively. Green and red outlines depict significantly negative and positive shift-score clusters ($p < 0.05$), respectively. **(E)** Shift scores of SOA 30 at 30 ms (green) and 0 ms (blue) temporal offset. Bars in the corresponding colours show significant shift scores ($p < 0.05$, cluster-corrected). Error-shading indicate 95 % C.I. of the mean. **(F)** Shift scores of SOA 45 at 45 ms (cyan) and 0 ms (blue) temporal offset.

### 3.5 Distinct temporal shifts of location processing stages during temporal integration

Average temporal shifts at each previously defined processing stage are shown in Table 1 and Figure 5. Apart from one exception, all confidence intervals of the temporal shifts fell in-between the onsets of Display 1 and 2. Group analyses showed that while the temporal shift was not significantly higher in the SOA 45 condition than the SOA 30 condition in the early processing stage (90 to 140 ms, $p = 0.146$), its average shift was higher in both the middle (140 to 300 ms, $p = 0.038$) and late processing stage (300 to 500 ms, $p < 0.001$).

| Time / Condition | 90 to 140 ms | 140 to 300 ms | 300 to 500 ms |
|---|---|---|---|
| SOA 30 | 16.5 ms (10-23 ms) | 9.5 ms (5.5-12.5 ms) | 17 ms (13.5-20 ms) |
| SOA 45 | 24 ms (12.5-33 ms) | 14 ms (5.5-20 ms) | 39.5 ms (28.5-53.5 ms) |

**Table 1.** Temporal shifts of location processing dynamics as a function of temporal integration condition (SOA 30/45), for each processing stage. 95% Confidence intervals are shown in brackets.

Pairwise comparisons between processing stages (averaged across both conditions) revealed that the temporal shift at the middle processing stage was significantly lower than at both the early and late processing stages ($p = 0.004$ and $p = 0.001$, respectively, Bonferroni-corrected), while the temporal shifts at the early and late stage did not differ significantly ($p > 0.5$, Bonferroni-corrected).

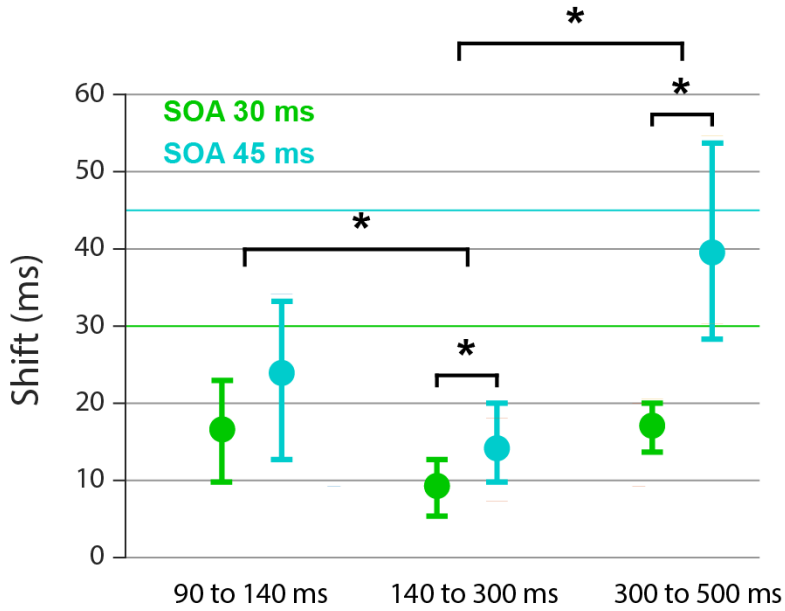


**Figure 5. Temporal shifts of location processing dynamics**

Error-bars are 95% C.I.s. Asterisks denote significant differences between SOAs and processing stages ($p < 0.05$, Bonferroni-corrected for comparisons between stages).

## 4 Discussion

We decoded the location of the missing element from EEG recorded in the temporal integration task that bears its name. This location is only apparent when the two successive stimulus displays in the missing element task are temporally integrated into a single perceptual representation, thus providing a highly time-sensitive fingerprint that can be tracked in the brain. We observed that perception is accelerated during temporal integration: The location of the missing element could be decoded sooner than would be expected on the basis of the actual delay between the stimulus displays. Compared to simultaneous presentation of the displays, the missing element was delayed by only 14 ms on average at an SOA of 30 ms (corresponding to an acceleration of 16 ms). At an SOA of 45 ms, the missing element was delayed by only 26 ms on average (19 ms acceleration). These results constitute evidence that the perception of the first display facilitated that of the second, thereby possibly aiding in their joint integration.

Importantly, the observed acceleration varied depending on the precise moment in the perceptual processing pathway. Combined across SOAs, processing was accelerated by 17 ms in the early stage, by 26 ms in the middle stage, and by 9 ms in the late stage. Thus, perceptual acceleration was neither linear, nor constant, but variable to the extent that early gains were at least partially lost again later. This variability suggests that as information flows from one processing stage to the next, it can wax as well as wane.

### 4.1 The locus of perceptual acceleration

In our experimental task, processing the second display was facilitated only by the onset of the first, less than 50 ms prior, which is an interval that has been considered too short to afford proper temporal preparation (Los & Schut, 2008). Indeed, at this temporal offset, the acceleration effect would seem to be driven purely by low-level factors within local neuronal assemblies in early visual cortex, such as synaptic facilitation (Markram et al., 1997; Zucker & Regehr, 2002). From this perspective, it is all the more surprising that the acceleration effect on the resultant representation was not straightforward (e.g., constant or linear). Such variable acceleration might be more expected when it is caused by higher-level factors (e.g., familiarity), which might arrive too late to interact with all processing stages, unlike the present manipulation.

The existence of variable perceptual acceleration is compatible with the general idea that perceptual and/or cognitive processing can be characterized by a certain order of operations (stages). The observed non-uniformity in the chaining of these operations might be conceptualized as a queuing effect that may happen when information is passed from one stage to another. In other words, rapid completion of processing in one stage may be followed by increased waiting time for the next stage. This concurrent variability between stages may alternatively originate from processes that occur in parallel, which complicates more

straightforward accounts of perceptual processing based on strictly serial stages (for an extended discussion see Caplan, 2009). To salvage the interpretability of stage-based models, flexible, data-driven approaches to identifying common processing stages, as well as their onsets and durations, may currently hold the most promise (e.g., Anderson et al., 2016; van Maanen, Portoles, & Borst, 2021; Vidaurre, Cichy, & Woolrich, 2021; Vidaurre et al., 2019).

As a caveat, it must be noted that the stages we identified in the present data were not the result of systematic analyses of the EEG, because it was not our purpose to attempt such identification. We therefore do not want to overstate the stage-specific nature of the observed acceleration effects. In our study, the processing stages have an arbitrary element. Their main purpose was to provide a handle on different moments in what might as well be considered a continuous processing stream (cf. Fig 4c & d). Importantly, the conclusion that the representation of the missing element location exhibited varying degrees of acceleration across the interval under consideration is largely unaffected by whether stage boundaries might be drawn differently within.

### 4.2 Temporal integration

The missing element task is traditionally used to measure visual temporal integration, and we indeed observed the associated pattern of results, in which increasing SOA resulted in fewer correct reports of the missing element location. The electrophysiological results provided an intriguing view on how temporal integration may be facilitated in the brain. To reiterate, the missing element location emerged sooner than would be expected on the basis of the SOA between the displays. This suggests that the processing of the first and second stimulus gets temporally ‘compressed’ in the brain, which might give rise to an increased sense of simultaneity. This compression is not predicted by models of temporal integration (for a review, see Akyürek, 2025), which generally assume that integration is mostly a consequence

of coincidence of the processing of the second display with lingering representations of the first display, referred to as visible persistence, rather than any perceptual acceleration (Dixon & Di Lollo, 1994; Hogben & Di Lollo, 1974; Loftus & Irwin, 1998; Sperling, 1960). The current results suggest that perceptual acceleration may play a role in facilitating the impression of simultaneity and thereby enhance temporal integration as well.

### 4.3 Conclusion

In the missing element task, we found that perception of the first display accelerates the processing of the second, which may contribute to the process of temporal integration. Temporal generalization analyses of the EEG patterns associated with the representation of the missing element showed that this acceleration is neither linear nor constant, and varies from moment to moment in the perceptual processing chain. Although the results are still compatible with the general idea of a fixed chain of perceptual processing stages, they do suggest that attempts to isolate and time processing stage-specific effects may mischaracterize the actual flow of events.

## Data and Code availability

All data will be openly available on osf.io/kftjw upon peer-reviewed publication. The custom Matlab code that reproduces all results in this manuscript is available on github.com/mijowolff/Accelerating-perception-during-temporal-integration.

## Author Contributions

Michael J. Wolff: Conceptualisation, Methodology, Software, Validation, Formal analysis, Investigation, Data curation, Writing—original draft, Writing—review & editing, Visualisation.

Elkan G. Akyürek: Conceptualisation, Methodology, Writing—original draft, Writing—review & editing, Supervision, Project administration, Resources

## Declaration of Competing Interests

The authors declare no competing interests.

**References**

Akyürek, E. G. (2025). Temporal integration as an adaptive process in visual perception, attention, and working memory. *Neuroscience & Biobehavioral Reviews*. https://doi.org/10.1016/j.neubiorev.2025.106041

Akyürek, E. G., Kappelmann, N., Volkert, M., & van Rijn, H. (2017). What you see is what you remember: Visual chunking by temporal integration enhances working memory. *Journal of Cognitive Neuroscience*, *29*, 2025–2036. https://doi.org/10.1162/jocn_a_01175

Akyürek, E. G., Schubö, A., & Hommel, B. (2010). Fast temporal event integration in the visual domain demonstrated by event-related potentials. *Psychophysiology*, *47*, 512–522. https://doi.org/10.1111/j.1469-8986.2010.00962.x

Anderson, J. R., Zhang, Q., Borst, J. P., & Walsh, M. M. (2016). The discovery of processing stages: Extension of Sternberg's method. *Psychological Review*, *123*, 481–509. https://doi.org/10.1037/rev0000030

Caplan, D. (2009). Experimental design and interpretation of functional neuroimaging studies of cognitive processes. *Human Brain Mapping*, *30*, 59–77. https://doi.org/10.1002/hbm.20489

Cichy, R. M., Pantazis, D., & Oliva, A. (2014). Resolving human object recognition in space and time. *Nature Neuroscience*, *17*, 455–462. https://doi.org/10.1038/nn.3635

Coull, J. T., & Nobre, A. C. (1998). Where and when to pay attention: The neural systems for directing attention to spatial locations and to time intervals as revealed by both PET and fMRI. *Journal of Neuroscience*, *18*, 7426–7435. https://doi.org/10.1523/JNEUROSCI.18-18-07426.1998

Di Lollo, V. (1977). Temporal characteristics of iconic memory. *Nature*, *267*, 241–243. https://doi.org/10.1038/267241a0

De Maesschalck, R., Jouan-Rimbaud, D., & Massart, D. L. (2000). The Mahalanobis distance. *Chemometrics and Intelligent Laboratory Systems, 50*, 1–18. https://doi.org/10.1016/S0169-7439(99)00047-7

Dixon, P., & Di Lollo, V. (1994). Beyond visible persistence: An alternative account of temporal integration and segregation in visual processing. *Cognitive Psychology, 26*, 33–63. https://doi.org/10.1006/cogp.1994.1002

Donders, F. C. (1868). Over de snelheid van psychische processen (On the speed of mental processes). *Onderzoekingen gedaan in het Physiologisch Laboratorium der Utrechtsche Hoogeschool, 1868±1869, Tweede reeks, II*, 92±120.

Friston, K. (2005). A theory of cortical responses. *Philosophical Transactions of the Royal Society B, 360*, 815–836. http://doi.org/10.1098/rstb.2005.1622

Griffin, I. C., Miniussi, C., & Nobre, A. C. (2002). Multiple mechanisms of selective attention: Differential modulation of stimulus processing by attention to space or time. *Neuropsychologia, 40*, 2325–2340. https://doi.org/10.1016/S0028-3932(02)00087-8

Hillyard, S.A., Teder-Sälejärvi, W.A., Münte, T.F. (1998). Temporal dynamics of early perceptual processing. *Current Opinion in Neurobiology, 8*, 202–210. https://doi.org/10.1016/S0959-4388(98)80141-4

Hogben, J. H., & Di Lollo, V. (1974). Perceptual integration and perceptual segregation of brief visual stimuli. *Vision Research, 14*, 1059–1069. https://doi.org/10.1016/0042-6989(74)90202-8

Jepma, M., Wagenmakers, E.-J., & Nieuwenhuis, S. (2012). Temporal expectation and information processing: A model-based analysis. *Cognition, 122*, 426–441. https://doi.org/10.1016/j.cognition.2011.11.014

Jones, M. R., Moynihan, H., MacKenzie, N., & Puente, J. (2002). Temporal aspects of stimulus-driven attending in dynamic arrays. *Psychological Science, 13*, 313–319. https://doi.org/10.1111/1467-9280.00458

King, J-R., & Dehaene, S. (2014). Characterizing the dynamics of mental representations: The temporal generalization method. *Trends in Cognitive Sciences, 18*, 203–210. https://doi.org/10.1016/j.tics.2014.01.002

Kirchner, H., & Thorpe, S. J. (2006). Ultra-rapid object detection with saccadic eye movements: Visual processing speed revisited. *Vision Research, 46*, 1762–1776. https://doi.org/10.1016/j.visres.2005.10.002

Kleiner, M., Brainard, D., Pelli, D., Ingling, A., Murray, R., & Broussard, C. (2007). What's new in Psychtoolbox-3. *Perception, 36*, 1–16.

Linden, D. E. (2007). What, when, where in the brain? Exploring mental chronometry with brain imaging and electrophysiology. *Reviews in the Neurosciences, 18*, 159–171. https://doi.org/10.1515/revneuro.2007.18.2.159

Ledoit, O., & Wolf, M. (2004). Honey, I shrunk the sample covariance matrix. *The Journal of Portfolio Management, 30*, 110–119. https://doi.org/10.3905/jpm.2004.110

Loftus, G. R., & Irwin, D. E. (1998). On the relations among different measures of visible and informational persistence. *Cognitive Psychology, 35*, 135–199. https://doi.org/10.1006/cogp.1998.0678

Los, S. A., & Schut, M. L. J. (2008). The effective time course of preparation. *Cognitive Psychology, 57*, 20–55. https://doi.org/10.1016/j.cogpsych.2007.11.001

Luce, R. (1986). *Response times: Their role in inferring elementary mental organization*. New York: Oxford University Press.

Mangun, G.R. (1995). Neural mechanisms of visual selective attention. *Psychophysiology, 32*, 4–18. https://doi.org/10.1111/j.1469-8986.1995.tb03400.x

Mangun, G. R., & Hillyard, S. A. (1991). Modulations of sensory-evoked brain potentials indicate changes in perceptual processing during visual-spatial priming. *Journal of Experimental Psychology: Human Perception and Performance*, *17*(4), 1057–1074. https://doi.org/10.1037/0096-1523.17.4.1057

Markram, H., Lübke, J., Frotscher, M., & Sakmann, B. (1997). Regulation of synaptic efficacy by coincidence of postsynaptic APs and EPSPs. *Science*, *275*, 213–215. https://doi.org/10.1126/science.275.5297.213

Marti, S., King, J.-R., & Dehaene, S. (2015). Time-resolved decoding of two processing chains during dual-task interference. *Neuron*, *88*, 1297–1307. https://doi.org/10.1016/j.neuron.2015.10.040

Mathewson, K. E., Fabiani, M., Gratton, G., Beck, D. M., & Lleras, A. (2010). Rescuing stimuli from invisibility: Inducing a momentary release from visual masking with pre-target entrainment. *Cognition*, *115*, 186–191. https://doi.org/10.1016/j.cognition.2009.11.010.

Myers, N. E., Rohenkohl, G., Wyart, V., Woolrich, M. W., Nobre, A. C., & Stokes, M. G. (2015). Testing sensory evidence against mnemonic templates. *eLife*, *4*, e09000. https://doi.org/10.7554/eLife.09000

Palmer, S. E., Marre, O., Berry, M. J., & Bialek, W. (2015). Predictive information in a sensory population. *Proceedings of the National Academy of Sciences USA*, *112*, 6908–6913. https://doi.org/10.1073/pnas.1506855112

Patel, S. H., & Azzam, P. N. (2005). Characterization of N200 and P300: Selected studies of the event-related potential. *International Journal of Medical Sciences*, *2*, 147–154. https://doi.org/10.7150/ijms.2.147

Polich, J. (2007). Updating P300: An integrative theory of P3a and P3b. *Clinical Neurophysiology*, *118*, 2128–2148. https://doi.org/10.1016/j.clinph.2007.04.019

Posner, M. I. (1980). Orienting of attention. *Quarterly Journal of Experimental Psychology*, *32*, 3–25. https://doi.org/10.1080/00335558008248231

Praamstra, P., Kourtis, D., Kwok, H. F., & Oostenveld, R. (2006). Neurophysiology of implicit timing in serial choice reaction-time performance. *Journal of Neuroscience*, *26*, 5448–5455. https://doi.org/10.1523/JNEUROSCI.0440-06.2006

Ridderinkhof, K. R., van der Molen, M. W., & Bashore, T. R. (1995). Limits on the application of additive factors logic: Violations of stage robustness suggest a dual-process architecture to explain flanker effects on target processing. *Acta Psychologica*, *90*, 29–48. https://doi.org/10.1016/0001-6918(95)00031-O

Rohenkohl, G., & Nobre, A. C. (2011). Alpha oscillations related to anticipatory attention follow temporal expectations. *Journal of Neuroscience*, *31*, 14076–14084. https://doi.org/10.1523/JNEUROSCI.3387-11.2011

Sackur, J., & Dehaene, S. (2009). The cognitive architecture for chaining of two mental operations. *Cognition*, *111*, 187–211. https://doi.org/10.1016/j.cognition.2009.01.010

Seibold, V. C., Bausenhart, K. M., Rolke, B., & Ulrich, R. (2011). Does temporal preparation increase the rate of sensory information accumulation? *Acta Psychologica*, *137*, 56–64, https://doi.org/10.1016/j.actpsy.2011.02.006

Seibold, V. C., Fiedler, A., & Rolke, B. (2011). Temporal attention shortens perceptual latency: A temporal prior entry effect. *Psychophysiology*, *48*, 708–717. https://doi.org/10.1111/j.1469-8986.2010.01135.x

Seibold, V. C., & Rolke, B. (2014). Temporal preparation and visual processing. *Psychophysiology*, *51*, 529–538. https://doi.org/10.1111/psyp.12196

Sperling, G. (1960). The information available in brief visual presentations. *Psychological Monographs: General and Applied*, *74*, 1–29. https://doi.org/10.1037/h0093759

Sternberg, S. (1969). The discovery of processing stages: Extensions of Donders' method. *Acta Psychologica*, *30*, 276-315. https://doi.org/10.1016/0001-6918(69)90055-9

Sternberg, S. (2001). Separate modifiability, mental modules, and the use of pure and composite measures to reveal them. *Acta Psychologica*, *106*, 147–246. https://doi.org/10.1016/s0001-6918(00)00045-7

Summerfield, C., & Egner, T. (2009). Expectation (and attention) in visual cognition. *Trends in Cognitive Sciences*, *13*, 403–409. https://doi.org/10.1016/j.tics.2009.06.003

Thorpe, S., Fize, D., & Marlot, C. (1996). Speed of processing in the human visual system. *Nature*, *381*, 520–522. https://doi.org/10.1038/381520a0

van Maanen, L., Portoles, O., & Borst, J.P. (2021). The discovery and interpretation of evidence accumulation stages. *Computational Brain & Behavior*, *4*, 395–415. https://doi.org/10.1007/s42113-021-00105-2

Vangkilde, S., Coull, J. T., & Bundesen, C. (2012). Great expectations: Temporal expectation modulates perceptual processing speed. *Journal of Experimental Psychology: Human Perception and Performance*, *38*, 1183–1191. https://doi.org/10.1037/a0026343

VanRullen, R., Thorpe, S. J. (2001). The time course of visual processing: From early perception to decision-making. *Journal of Cognitive Neuroscience*, *13*, 454–461. https://doi.org/10.1162/08989290152001880

Vidaurre, D., Cichy, R. M., & Woolrich, M. W. (2021). Dissociable components of information encoding in human perception. *Cerebral Cortex*, *31*, 5664–5675. https://doi.org/10.1093/cercor/bhab189

Vidaurre, D., Myers, N. E., Stokes, M., Nobre, A. C., & Woolrich, M. W. (2019). Temporally unconstrained decoding reveals consistent but time-varying stages of stimulus processing. *Cerebral Cortex*, *29*, 863–874. https://doi.org/10.1093/cercor/bhy290

Verleger, R., Jaśkowski, P., Wascher, E. (2005). Evidence for an integrative role of P3b in linking reaction to perception. *Journal of Psychophysiology, 19*, 165–181. https://doi.org/10.1027/0269-8803.19.3.165

Vogel, E. K., & Machizawa, M. G. (2004). Neural activity predicts individual differences in visual working memory capacity. *Nature, 428*, 748–751. https://doi.org/10.1038/nature02447

Woldorff, M. G., Fox, P. T., Matzke, M., Lancaster, J. L., Veeraswamy, S., Zamarripa, F., Seabolt, M., Glass, T., Gao, J. H., Martin, C. C., & Jerabek, P. (1997). Retinotopic organization of early visual spatial attention effects as revealed by PET and ERPs. *Human Brain Mapping, 5*, 280–286. https://doi.org/10.1002/(SICI)1097-0193(1997)5:4<280::AID-HBM13>3.0.CO;2-I

Wolff, M.J., Ding, J., Myers, N.E., & Stokes, M. G. (2015). Revealing hidden states in visual working memory using electroencephalography. *Frontiers in Systems Neuroscience, 9*, 123. https://doi.org/10.3389/fnsys.2015.00123.

Zucker, R. S., & Regehr, W. G. (2002). Short-term synaptic plasticity. *Annual Review of Physiology, 64*, 355–405. https://doi.org/10.1146/annurev.physiol.64.092501.114547